

Convex Combination Consistency between Neighbors for Weakly-supervised Action Localization

Qinying Liu, Zilei Wang*, Ruoxi Chen, Zhilin Li

Department of Automation, University of Science and Technology of China
{lydyc, ruoxi16, lizhilin}@mail.ustc.edu.cn, zlwang@ustc.edu.cn

Abstract

In weakly-supervised temporal action localization (WS-TAL), the methods commonly follow the “localization by classification” procedure, which uses the snippet predictions to form video class scores and then optimizes a video classification loss. In this procedure, the snippet predictions (or snippet attention weights) are used to separate foreground and background. However, the snippet predictions are usually inaccurate due to absence of frame-wise labels, and then the overall performance is hindered. In this paper, we propose a novel C³BN to achieve robust snippet predictions. C³BN includes two key designs by exploring the inherent characteristics of video data. First, because of the natural continuity of adjacent snippets, we propose a micro data augmentation strategy to increase the diversity of snippets with convex combination of adjacent snippets. Second, we propose a macro-micro consistency regularization strategy to force the model to be invariant (or equivariant) to the transformations of snippets with respect to video semantics, snippet predictions and snippet features. Experimental results demonstrate the effectiveness of our proposed method on top of baselines for the WS-TAL tasks with video-level and point-level supervision.

1 Introduction

Temporal action localization (TAL) is a task to localize the start and end timestamps of action instances and recognize their categories. In recent years, many works put effort into the fully supervised manner and gain great achievements. However, these fully supervised methods require extensive manual frame level annotations. To address this problem, many weakly-supervised TAL (dubbed WS-TAL) methods are proposed to explore an efficient way to detect the action instances in the given videos with only weak supervision. Among diverse weak supervisions, video-level labels are the most commonly used.

Most existing methods formulate the WS-TAL as a video action recognition problem. Specifically, each input video is first transformed into snippet features, then the snippet-wise classifications are calculated to generate a temporal class activation sequence (T-CAS). Since only the video action labels are known, they aggregate scores from snippets with high probabilities of belonging to the action to form a video classification score. There are two main strategies for this purpose: multi-instance learning (MIL) [Lee *et al.*, 2020] or attention mechanism [Huang *et al.*, 2021]. The former strategy obtains video-level class scores from T-CAS by applying a pooling on the top-k values for each class. The later strategy introduces snippet attention weights to highlight action snippets and eliminate irrelevant background snippets. Both strategies end up with a classification loss using video labels. Despite of the efforts, the performances of these methods rely on the quality of the snippet-level predictions (including the attention weights). However, in absence of frame-level supervision, it is difficult for the WS-TAL models to obtain accurate snippet predictions.

In this paper, we propose a simple yet effective training strategy dubbed Convex Combination Consistency Between Neighbors (C³BN), which aims to achieve robust snippet predictions. The core idea of C³BN is to leverage the inherent smoothness within the videos to perform effective model regularization. By ‘smoothness’, we mean that the scenes in real-world video usually change smoothly. Based on this, we propose a micro¹ data augmentation strategy, where we mix the pairs of adjacent snippets (dubbed *parent snippets*) by convex combination and generate a set of new snippets (dubbed *child snippets*). The operation is borrowed from MixUp [Zhang *et al.*, 2018], but there are some task-specific insights. Specifically, due to the natural smoothness within videos, the child snippets have two important properties. 1) They are similar to realistic snippets, since the adjacent snippets are usually visually similar. 2) Their temporal locations lie in-between the parent snippets. More importantly, compared with the parent snippets, the child snippets have more diverse temporal locations. These two properties give the potential for exploring more patterns in-between adjacent snippets in the latent representations, thereby boosting the generalization power of the

¹By ‘micro’, we mean the proposed data augmentation strategy is for snippets rather than videos.

*Corresponding author

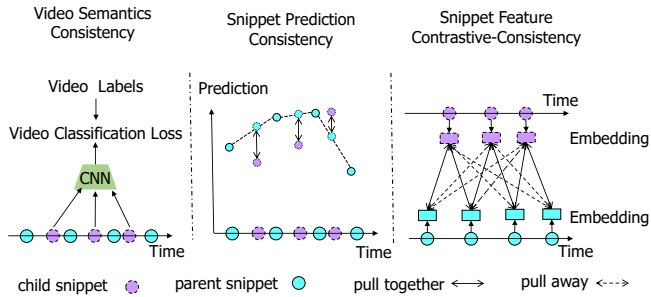


Figure 1: **Illustration of different consistency regularization.**

model to data points in-between adjacent snippets.

One natural question to ask arises: how to leverage the child snippets for model regularization during training? To achieve this goal, we design the macro-micro consistency regularization strategy (shown in Figure 1), aiming to enable the model to possess three desired properties. 1) Video semantics consistency or invariance. We compute the video classification loss on the child snippet sequences, making the video-level semantics of the child snippets consistent with the original one. Since the child snippets are more ambiguous, the model is forced to pay more attention to non-salient action snippets, thereby reducing false alarms of background. 2) Snippet prediction consistency or equivariance. Based on the natural smoothness within video, we argue the model should also perform smoothly in-between adjacent snippets. That’s, we enforce the prediction of a child snippet to be consistent with the same convex combination of predictions of its parent snippets. This regularization has two advantages. First, it forces the model to learn a flat decision boundary between adjacent snippets, which can improve the stability of predictions of perturbed snippets, thereby leading to preciser action boundary localization on a held-out test dataset. Second, it enables less variation across adjacent snippets/visually similar snippets, thereby resulting in more continuous predictions in temporal dimension. 3) Snippet feature contrastive-consistency. Inspired by image clustering [Do *et al.*, 2021] that the representation learning is complementary to classifier learning, we propose to further regularize the intermediate features of the model. More importantly, we integrate the feature consistency regularization into the contrastive learning scheme. With the help of instance (*i.e.*, snippet) discrimination, the model can retain the information for identifying the fine details that separate snippets, which are particularly desired for foreground and background separation within a video. By further imposing the consistency constraint, the representations are further learned to automatically group semantically similar snippets together. To simultaneously achieve both, we introduce a soft version of InfoNCE-based contrastive loss. Besides, we design a bilateral reference mechanism where child and parent snippets are alternately queried.

The proposed C³BN is simple, flexible and universal. First, it is complementary to existing WS-TAL methods. We demonstrate that our method obtains significant improvement on a variety of base approaches and datasets. Besides, our method is suitable for incorporating with multi-scale test-

ing technique and earns a more significant performance gain compared with baselines. Finally, we extend our method to the point-supervised WS-TAL task and observe the same promotion in the performance. We summarize our contributions as follows:

- We propose a novel snippet augmentation strategy by convex combination between adjacent snippets, considering the critical role of adjacent snippets in WS-TAL task.
- We propose three regularization terms to enhance their consistency properties with respect to video semantics, snippet predictions and snippet features.
- The proposed strategy is generic and can be applied to various WS-TAL methods with video-level supervision and point-level supervision.

2 Related Work

Data Augmentation aims to enlarge the train set using transformations. Conventional image transformations include cropping, flips, rotation and *etc.* Recent studies consider employing multiple images for augmentation. MixUp [Zhang *et al.*, 2018] proposes to combine the pixel values and labels of two images by linear interpolation. It has been proven effective for the classification task, which is followed by [Verma *et al.*, 2019]. Our method employs the idea of instance mixtures with task-specific designs. Concretely, we achieve the mixture operation on two snippets within a video rather than on two different videos likewise MixUp, making the perturbations to snippets more controllable for incorporating the proposed method into the existing WS-TAL frameworks.

Consistency Regularization is crucial in semi-supervised learning (SSL). It is assumed that a classifier should output the same class probability for an unlabeled sample even after it is augmented. Prior works [Laine and Aila, 2017] apply the consistency regularization loss on different augmentations of an unlabeled sample. After that, several variants [Berthelot *et al.*, 2019; Sohn *et al.*, 2020] are further proposed to extend its applications. Among them, [Berthelot *et al.*, 2019] also uses MixUp by mixing unlabeled samples and their guessed labels. The main difference between our method and them is that we don’t guess the hard labels of unlabeled samples, thereby reducing undesirable noise.

Self-supervised Contrastive Learning has attracted much attention for pre-training. The widely adopted contrastive learning [Chen *et al.*, 2020; He *et al.*, 2020] optimizes the model by instance discrimination. Specifically, it learns to embed the features of differently augmented versions of the same image to be similar, while to be dissimilar if they came from different images. Some recent works [Kim *et al.*, 2020] have leveraged the idea of MixUp for contrastive learning. Our method is different from these methods in: (1) The above methods regard the mixed samples as queries and the original samples as keys, while we additionally consider a reverse operation to exchange their roles. (2) In our method, the negative samples come from the same video as the positive samples, they can be viewed as hard negative samples, which is important in contrastive learning [Robinson *et al.*, 2020].

Weakly-Supervised Temporal Action Detection aims to tackle temporal action localization in the weakly-supervised

setting. Video label is the most common supervision in practice. Most existing models follow the “localization by classification” procedure and aggregates frame class scores to produce video prediction. BaS-Net [Lee *et al.*, 2020] introduces an auxiliary class for background and suppress activations from background frames. Meanwhile, FAC-Net [Huang *et al.*, 2021] takes the foreground-action consistency into consideration and models the bilateral relations. Another method has noticed the contrastive learning. CoLA [Zhang *et al.*, 2021] forms hard-easy snippet contrastive pairs and conduct the feature refinement via their proposed contrastive loss. It is significantly differently from ours in that it relies on pseudo action labels for defining positive pairs and negative pairs, while we formula it as an instance discrimination task. Recently, point supervision becomes a new research hotspot. SF-Net [Ma *et al.*, 2020] mines pseudo action and background frames. Recently, LACP [Lee and Byun, 2021] improves performance by dense pseudo-labels that is likely to contain complete action instances.

3 Recap of WS-TAL methods

To be self-included, we first describe basic pipeline of mainstream methods which are used as our baselines.

Notations and Preliminaries For an untrimmed video V , we can only access its one-hot video label $\mathbf{y} = \{y_i\}_{i=1}^C$, where C represents the number of classes. Following the common practice, we first divide V into non-overlapping snippets, *i.e.*, $\mathbf{S} = \{s_t\}_{t=1}^T$. For each snippet s_t , we apply a pre-trained feature extractor to extract two feature vectors dubbed $\mathbf{f}_t^R, \mathbf{f}_t^O$ for RGB and optical-flow, respectively. Then we stack the sequences $\{\mathbf{f}_t^R\}_{t=1}^T$ and $\{\mathbf{f}_t^O\}_{t=1}^T$ to get a RGB feature map \mathbf{F}^R and a optical-flow feature map \mathbf{F}^O . Previous methods either concatenate \mathbf{F}^R and \mathbf{F}^O together or process \mathbf{F}^R and \mathbf{F}^O independently before feeding them into subsequent network. For simplicity, we use \mathbf{F} to represent the input feature sequence in the rest of this paper. Here $\mathbf{F} \in \mathbb{R}^{T \times D_f}$, and D_f is the channel dimension.

Feature Embedding Since the extracted features \mathbf{F} are not trained from scratch for the W-TAL task, the mainstream methods further introduce a feature embedding module to map the extracted video feature to task-specific feature space. Concretely, they usually apply a few 1D convolution layers to map the original features $\mathbf{F} \in \mathbb{R}^{T \times D_f}$ to task-specific feature $\mathbf{E} = [e_1, \dots, e_T] \in \mathbb{R}^{T \times D_e}$.

Snippet Classification To localize action instances, mainstream methods compute T-CAS from embedded feature \mathbf{E} . Specifically, they feed \mathbf{E} into a snippet classifier with $C + 1$ classes to predict snippet classification *logit* scores $\mathbf{S} = [s_1, \dots, s_T] \in \mathbb{R}^{T \times (C+1)}$, where each snippet has its own classification scores $s_t = [s_{t,1}, \dots, s_{t,C+1}] \in \mathbb{R}^{C+1}$. Note that, the $(C + 1)$ -th class denotes the background class.

Video Classification Since we only have the video labels, we first aggregate the snippet scores to obtain video class scores for computing a video classification loss. There are two main strategies in the literature to obtain video scores: MIL-based methods and attention-based methods. Without

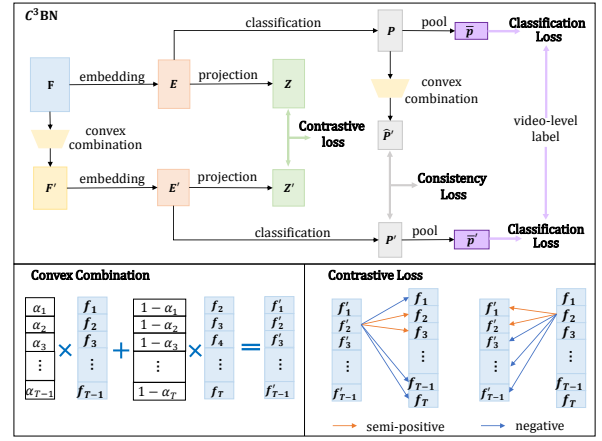


Figure 2: **The overview of our proposed C^3BN .** We first perform convex combination on input snippet features \mathbf{F} to produce augmented snippet feature \mathbf{F}' . The procedure is denoted as micro data augmentation. Then we simultaneously feed the \mathbf{F} and \mathbf{F}' into the model and compute four regularization loss terms. We call the procedure macro-micro consistency regularization.

loss of generality, we only review the basic pipeline of MIL-based methods in the paper.

These methods average the top- k snippet scores along temporal dimension for each class to build the video class score:

$$\bar{s}_c = \frac{1}{k} \max_{l \subset \{1, \dots, T\}, |l|=k} \sum_{\tau \in l} s_{\tau, c} \quad \forall c \in \{1, \dots, C + 1\}, \quad (1)$$

where k is a hyper-parameter proportional to the video length T , *i.e.*, $k = \max(1, T//r)$, and r is a pre-defined parameter. Thereafter, we obtain the probability for each class by applying the Softmax function to the aggregated scores:

$$\bar{p}_c = \frac{\exp(\bar{s}_c)}{\sum_{i=1}^{C+1} \exp(\bar{s}_i)} \quad \forall c \in \{1, \dots, C + 1\}, \quad (2)$$

Finally we formulate the video classification loss as

$$\mathcal{L}_{cls} = -\frac{1}{C + 1} \sum_{c=1}^{C+1} \bar{y}_c \log \bar{p}_c, \quad (3)$$

where $\bar{\mathbf{y}} = [y_1, \dots, y_C, 1] \in \mathbb{R}^{C+1}$. The label for background class is set to be 1 since all training videos contain background frames.

4 Our Method

In this section, we introduce our proposed C^3BN . The overview of our proposed C^3BN is shown in Figure 2. There are two procedures in C^3BN , including the micro data augmentation and macro-micro consistency regularization.

4.1 Micro Data Augmentation

Upon the original T snippet features $\{\mathbf{f}_t\}_{t=1}^T$, we perform convex combination on adjacent snippet features to generate augmented snippet features Formally,

$$\mathbf{f}'_{t,\tau} = \alpha \mathbf{f}_t + (1 - \alpha) \mathbf{f}_{t+\tau}, \quad (4)$$

where $\mathbf{f}'_{t,\tau}$ is the child snippet and $\{\mathbf{f}_t, \mathbf{f}_{t+\tau}\}$ are the parent snippets. The weight $\alpha \in (0, 1)$ is randomly sampled from a beta distribution $\text{Beta}(\gamma, \gamma)$. Here γ is a preset positive scalar. The τ is temporal distance with $\tau \in \{1, \dots, T_M\}$, where T_M is the maximum distance of two adjacent snippets with $T_M \ll T$. In this paper, we empirically set T_M to 1. Then for the snippet sequence with length T , we can obtain $T - 1$ child snippets as follows

$$\mathbf{f}'_t = \alpha_t \mathbf{f}_t + (1 - \alpha_t) \mathbf{f}_{t+1} \quad \forall t \in \{1, \dots, T - 1\}, \quad (5)$$

where $\alpha = [\alpha_1, \dots, \alpha_{T-1}] \in \mathbb{R}^{T-1}$ are different random weights. The child snippets $\{\mathbf{f}'_t\}_{t=1}^{T-1}$ are concatenated to form a feature map dubbed $\mathbf{F}' \in \mathbb{R}^{(T-1) \times D_f}$.

4.2 Macro-Micro Consistency Regularization

To make the child snippets participate in training to cooperate with parent snippets, we introduce three regularization terms to jointly regularize the learning procedure.

Video Semantic Consistency Compared with the original \mathbf{F} , \mathbf{F}' is a locally shifted version while the video semantics should remain unchanged. Thus, we can feed the \mathbf{F}' into network and get a video classification loss in the same form as L_{cls} . We denote the loss by L'_{cls} . Obviously, the child snippet sequence is harder to recognize, then the model is forced to discover action snippets from the 'non-salient' region. It is helpful to avoid the model focuses on only a few discriminative snippets, thereby improving the snippet classification accuracy. However, such macro regularization ignores the fine relationships between child snippets and parent snippets. To this end, we propose to further regularize the network from more micro perspective.

Snippet Prediction Consistency It has been shown in SSL that the conditional probability distribution varies smoothly along the manifold of its marginal distribution [Belkin *et al.*, 2006]. Here, we assume that similar conclusion holds for our case, *i.e.*, the model should output smooth predictions for data points in-between adjacent snippets. Besides, such property is consistent with the natural smoothness of videos. Specifically, we first normalize the snippet logit scores \mathbf{S} with a Softmax operation as,

$$\mathbf{P} = \text{Softmax}(\mathbf{S}) \quad (6)$$

where $\mathbf{P} = [\mathbf{p}_1, \dots, \mathbf{p}_T] \in \mathbb{R}^{T \times (C+1)}$ is the the normalized sequence. By feeding \mathbf{F}' into the same network, we can obtain another score sequence dubbed \mathbf{P}' . To bridge the \mathbf{P} and \mathbf{P}' , we apply convex combination on \mathbf{P} to obtain the shifted version of \mathbf{P} dubbed $\hat{\mathbf{P}}'$. Formally,

$$\hat{\mathbf{p}}'_t = \alpha_t \mathbf{p}_t + (1 - \alpha_t) \mathbf{p}_{t+1} \quad \forall t \in \{1, \dots, T - 1\}, \quad (7)$$

Then we apply the MSE loss to enforce the consistency between \mathbf{P}' and $\hat{\mathbf{P}}'$. Formally,

$$\mathcal{L}_{cons} = \frac{1}{T-1} \sum_{t=1}^{T-1} \|(\mathbf{p}'_t - \hat{\mathbf{p}}'_t) \cdot \bar{\mathbf{y}}\|_2^2, \quad (8)$$

Here we only calculate the loss on the classes presented in video label $\bar{\mathbf{y}}$ to avoid confusing the model with irrelevant

classes. As for the irrelevant classes, a natural idea is to suppress their predicted scores in \mathbf{P} and \mathbf{P}' , which has been achieved by L_{cls} and L'_{cls} . Note that, in attention-based methods, the attention weights can be regarded as foreground scores, thus we should also compute the same form of consistency loss for them.

Snippet Feature Contrastive-Consistency This regularization is imposed in the snippet feature space. By 'consistency', we mean that we enforce the model to learn the relative similarity of representations, reflecting how much each child snippet has the parent snippets. By 'contrastive', we mean that the model should be able to distinguish the parent snippets of each child snippet from other parent snippets. We jointly achieve them here.

Specifically, following convention [Chen *et al.*, 2020], we first employ a projection head consisting of a FC layer and a L2 normalization for mapping the embed feature \mathbf{E} into a low-dimensional unit hypersphere. We express the output as $\mathbf{Z} = [z_1, \dots, z_t] \in \mathbb{R}^{T \times D_z}$. Here D_z is the number of channels with $D_z < D_f$. Likewise, we can also obtain the compact representations of \mathbf{E}' denoted by $\mathbf{Z}' = [z'_1, \dots, z'_t]$.

Taking each child snippet z'_t as query, we can define that: 1) its parent snippets z_t and z_{t+1} are two semi-positive keys with the probability of α_t and $1 - \alpha_t$, respectively. 2) other snippets in \mathbf{Z} are negative keys. Thus we can construct a soft contrastive loss as

$$\mathcal{L}_{cont} = -\frac{1}{T-1} \sum_{t=1}^{T-1} \alpha_t \log \frac{\exp(z'^{\top}_t z_t / \rho)}{\sum_{\tau=1}^T \exp(z'^{\top}_t z_{\tau} / \rho)} + (1 - \alpha_t) \log \frac{\exp(z'^{\top}_t z_{t+1} / \rho)}{\sum_{\tau=1}^T \exp(z'^{\top}_t z_{\tau} / \rho)}, \quad (9)$$

where ρ is the temperature coefficient.

Eq.(9) only considers the unilateral reference from \mathbf{Z} to \mathbf{Z}' . To explore more fine-grained patterns and also enforce the consistency regularization between \mathbf{Z} and \mathbf{Z}' , we propose a bilateral reference mechanism to further take the reference from \mathbf{Z}' to \mathbf{Z} into consideration. That's, we treat the elements of \mathbf{Z} as queries and the elements of \mathbf{Z}' as keys. Meanwhile, snippet-to-snippet relations remain unchanged. Thus, we can compute another contrastive loss dubbed \mathcal{L}'_{cont} likewise Eq.(9). Here, we omit the details.

Training Objective To train the entire model in an end-to-end fashion, we optimize the following loss function:

$$\mathcal{L} = \mathcal{L}_{base} + \lambda_1 \mathcal{L}'_{cls} + \lambda_2 \mathcal{L}_{cons} + \lambda_3 (\mathcal{L}_{cont} + \mathcal{L}'_{cont}). \quad (10)$$

where λ_* denotes the weight term. The $\mathcal{L}_{base} = \mathcal{L}_{cls} + \mathcal{L}_{other}$ represents the objective function of the baseline, where \mathcal{L}_{other} represents the sum of other losses apart from \mathcal{L}_{cls} .

Multi-Scale Testing Our method is inherently capable of handling resized videos, because the linear interpolation of the whole video can be regarded as a special case of our method. Thus we also compare the performances of our method and baselines when using the multi-scale testing, a popular technique in object detection [Zhou *et al.*, 2019]. That's, we first resize each video sequence to several preset scales and then input them into the model one by one. Finally, we ensemble their detection results.

Method	0.3	0.5	0.7	Avg
A2CL [Min and Corso, 2020]	48.1	30.1	10.6	29.4
ACSNet [Liu <i>et al.</i> , 2021]	51.4	32.4	11.7	32.0
AUMN [Luo <i>et al.</i> , 2021]	54.9	33.3	9.0	32.4
UGCT [Yang <i>et al.</i> , 2021]	55.5	35.9	11.4	34.6
CoLA [Zhang <i>et al.</i> , 2021]	51.5	32.2	13.1	32.1
D2-Net [Narayan <i>et al.</i> , 2021]	52.3	36.0	-	-
CSCL [Ji <i>et al.</i> , 2021]	52.7	33.4	12.3	32.7
BaS-Net [Lee <i>et al.</i> , 2020]*	43.0	26.1	9.4	26.1
+ C ³ BN	44.9	28.5	11.4	28.3(+2.2)
BaS-Net*†	44.3	26.9	9.9	27.0
+ C ³ BN	47.4	29.7	11.9	29.6(+2.6)
FAC-Net [Huang <i>et al.</i> , 2021]*	52.6	32.8	12.3	32.5
+ C ³ BN	53.1	34.6	13.0	33.7(+1.2)
FAC-Net*†	54.8	33.8	12.4	33.4
+ C ³ BN	55.5	35.9	13.4	35.2(+1.8)

Table 1: The comparison on the THUMOS14 in terms of mAP at tIoU thresholds [0.3 : 0.7 : 0.1]. * indicates that the result is based on our re-implementation. '†' denotes using multi-scale testing.

Method	0.50	0.75	0.95	Avg
A2CL [Min and Corso, 2020]	36.8	22.5	5.2	22.5
ACSNet [Liu <i>et al.</i> , 2021]	36.3	24.2	5.8	23.9
AUMN [Luo <i>et al.</i> , 2021]	38.3	23.5	5.2	23.5
UGCT [Yang <i>et al.</i> , 2021]	39.1	22.4	5.8	23.8
BaSNet [Lee <i>et al.</i> , 2020]*	35.6	21.0	5.3	21.7
+C ³ BN	37.3	22.4	5.4	23.0(+1.3)
FAC-Net [Huang <i>et al.</i> , 2021]*	40.1	24.2	5.8	24.7
+C ³ BN	45.2	26.9	5.9	27.3(+2.6)

Table 2: The performance comparison on the ActivityNet1.3 in terms of mAP at tIoU thresholds [0.5 : 0.95 : 0.05].

5 Experiments

In this section, we validate the effectiveness of our proposed C³BN. Due to the space constraint, we refer readers to Supplementary for more details for all experiments.

5.1 WS-TAL with Video Label

Datasets and Settings *THUMOS14* [Jiang *et al.*, 2014] contains untrimmed videos with 20 classes. We use the 200 videos in validation set for training and the 213 videos in testing set for evaluation. *ActivityNet13* [Caba Heilbron *et al.*, 2015] is a large-scale dataset with 200 categories. We train on the training set with 10,024 videos and test on validation set with 4,926 videos. We follow the standard evaluation protocol by reporting mean Average Precision (mAP) values under different temporal intersection over union (tIoU) thresholds.

Effectiveness of C³BN on Different Baselines To validate the generic effectiveness of C³BN, we incorporate C³BN into different WS-TALs as our baselines, including BaS-Net [Lee *et al.*, 2020] and FAC-Net [Huang *et al.*, 2021]. Note that, the BaS-Net is basically a MIT-based method, while FAC-Net mainly adopts the attention-based formula. Table 1 and Table 2 show the comparisons. C³BN consistently improves the performances of both baselines, regardless of the differences on the baselines and datasets.

id	\mathcal{L}_{base}	\mathcal{L}'_{cls}	\mathcal{L}_{cons}	\mathcal{L}_{cont}	\mathcal{L}'_{cont}	RGB	Flow
1	✓					17.7	30.6
2	✓	✓				18.4	30.9
3	✓		✓			18.4	31.2
4	✓			✓	✓	18.6	31.0
5	✓	✓	✓			18.7	31.5
6	✓	✓		✓	✓	19.9	31.5
7	✓		✓	✓	✓	18.8	31.7
8	✓	✓	✓		✓	19.7	31.8
9	✓	✓	✓	✓		19.6	31.7
10	✓	✓	✓	✓	✓	20.0	32.0

Table 3: Ablation studies on the THUMOS14, where average mAP at tIoU thresholds [0.3 : 0.7 : 0.1] is reported. The 'id' denotes the index of the model.

FAC-Net+C ³ BN	F-Drop ($p_{drop}=?$)			F-Noise ($n_{noise}=?$)			F-Mix (ours)
	0.1	0.3	0.5	0.1	0.3	0.5	—
RGB	18.1	17.7	17.3	18.3	17.6	16.7	20.0

Table 4: Comparison between different augmentation techniques.

Analysis of Loss Terms of C³BN Our C³BN introduces several additional loss terms during training. To figure out the contribution of each loss term, we conduct detailed ablation study in Table 3. The experiments are conducted on FAC-Net. FAC-Net independently processes RGB stream and Flow stream during training, which enables us to investigate the generalization ability of C³BN in different data modalities. The results demonstrate that 1) Each loss term alone can improve the performance (see model 1-4), indicating that all the regularizations are helpful. 2) Combining any two terms can consistently improve the performance, demonstrating the complementary relations among the loss terms (see model 5-7). 3) The combination of \mathcal{L}_{cont} and \mathcal{L}'_{cont} outperforms using only of them, verifying that effectiveness of our proposed cross-reference mechanism (see model 8-9). Moreover, above observations are consistent for both RGB and Flow streams, which further proves the effectiveness of C³BN.

Effectiveness of Convex Combination In the paper, we propose to achieve data augmentation through convex combination of adjacent snippets. To examine our design, we also investigate two other popular data augmentation techniques. 1) 'F-Drop': we randomly drop some activations of input features \mathbf{F} with probability of p_{drop} . 2) 'F-Noise': we randomly sample a noise tensor \mathbf{N} of the same size as \mathbf{F} from the uniform distribution $\mathbf{N} \sim \mathcal{U}(-n_{noise}, n_{noise})$, and the noise is injected into \mathbf{F} via $\mathbf{F}' = (\mathbf{F} \odot \mathbf{N}) + \mathbf{F}$. By convention, we assume that the F-Noise and F-Drop won't change the semantics of each individual snippet. Thus, when adapting the C³BN to F-Noise and F-Drop, we enforce the model to give same prediction for each original snippet and augmented snippet. Besides, in feature contrastive learning, each original snippet and its augmented snippet are positive. The comparison between F-Drop, F-Noise, and our method (termed as F-Mix) is shown in Table 4, where the RGB stream of FCA-Net is evaluated. It can be seen that our method significantly outperforms both F-Noise and F-Drop. It is because that F-

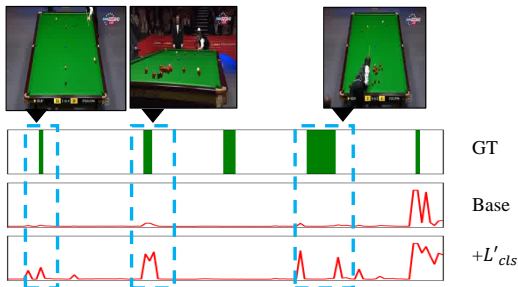


Figure 3: Qualitative results on THUMOS14. We show the T-CAS without and with macro consistency regularization.

Noise and F-Drop may change the semantics of the snippets, especially for the snippet near the decision boundary. Thus it will violate aforementioned assumption and harm the performance. In contrast, our method allows the semantics of augmented snippets change smoothly, thereby resulting in flatten representations with stronger generalization ability.

Multi-Scale Testing As a side product, our C^3BN is compatible with multi-scale testing. In Table 1, we report the results with the multi-scale testing. It can be seen that 1) the multi-scale testing is very effective in improving performance for either baselines and our methods. 2) After equipped with C^3BN , the performance gains of multi-scale testing become more significant, making C^3BN more applicable in reality.

Comparisons with State-of-the-Arts (SOTAs) To compare with previous SOTAs, we implement our C^3BN on recent strong WS-TAL method FAC-Net. Table 1 and Table 2 show the comparisons with previous approaches on THUMOS14 and ActivityNet1.3, respectively. From the results, we can see that FAC-Net+ C^3BN achieves the best performances on both datasets.

5.2 Visualization

To further validate the effectiveness of our method, we visualize some examples of the T-CAS *w.r.t* the video labels. We adopt the FAC-Net as our baseline. For more visualization examples, please refer to the Supplementary.

Effectiveness of Macro Consistency In Figure 3, the Base only activates the snippets of the rightmost action instance. It is because the video classification can be achieved by only a few salient snippets. Besides, \mathcal{L}'_{cls} is able to help mine more action snippets. The reason is that it is more difficult for the model to recognize each child snippet, and thus automatically aggregate information from more action regions.

Effectiveness of Micro Consistency As shown in Figure 4, we can see that the \mathcal{L}_{cons} and \mathcal{L}_{cont} (including \mathcal{L}'_{cont}) are helpful to suppress the responses of background and lead to a smoother T-CAS. We argue the reason is that the \mathcal{L}_{cont} and \mathcal{L}_{cons} enables the model to learn relative similarity between different snippets, and further to force the snippets from the same category closer together in both prediction space and feature space, thereby improving the foreground and background separation.

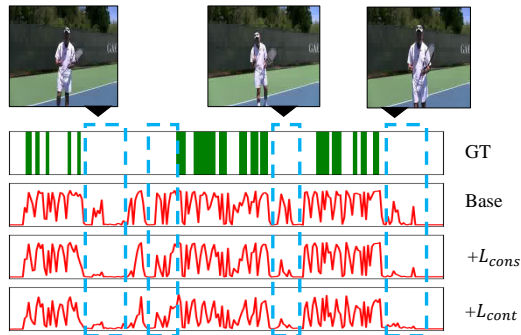


Figure 4: Qualitative results on THUMOS14. We show the T-CAS with and without micro consistency regularization.

Method	0.3	0.5	0.7	Avg
DC [Ju <i>et al.</i> , 2021]	58.1	34.5	11.9	34.5
SF-Net [Ma <i>et al.</i> , 2020]*	52.3	29.3	9.3	30.2
+ C^3BN	57.3	30.7	10.3	32.2(+2.0)
LACP [Lee and Byun, 2021]*	64.0	44.5	20.6	43.9
+ C^3BN	65.7	47.6	22.6	46.0(+2.1)

Table 5: The comparison on THUMOS14 in terms of mAP at tIoU thresholds [0.3 : 0.7 : 0.1].

5.3 WS-TAL with Point Label

The MIL-based scheme has also been exploited in WS-TALs with point supervision [Ma *et al.*, 2020], where the aforementioned issue still exists. Our C^3N is generic and is expected to work well for this task. We take SFNet [Ma *et al.*, 2020] and LACP [Lee and Byun, 2021] as the baselines, and conduct experiments on THUMOS14, BEOID [Calway *et al.*, 2015] and GTEA [Lei and Todorovic, 2018]. As shown in Table 5 and Table 6, our C^3BN strategy improves the mAP of the SF-Net and LACP by a large margin. Besides, our method also outperforms recent proposed DC [Ju *et al.*, 2021], and achieves SOTA performance on all three datasets. These validate that our C^3BN is compatible with WS-TAL with different weak supervisions.

Dataset	Method	0.1	0.3	0.5	0.7	Avg
GTEA	DC	59.7	38.3	21.9	18.1	33.7
	SF-Net*	53.8	38.0	21.9	18.2	32.3
	+ C^3BN	55.1	40.7	22.9	18.2	34.2(+1.9)
BEOID	DC	63.2	46.8	20.9	5.8	34.9
	SF-Net*	60.3	43.2	21.7	11.0	33.9
	+ C^3BN	65.5	44.0	26.3	9.7	37.0(+3.1)
	LACP*	81.4	73.1	45.8	21.7	56.6
+ C^3BN	82.1	73.3	47.4	23.3	57.6(+1.0)	

Table 6: The comparison on GTEA and BEOID in terms of mAP at tIoU thresholds [0.1 : 0.7 : 0.1].

6 Conclusion

In this paper, we propose a training strategy dubbed C^3BN to improve the snippet predictions. It first generates new snippets by convex combination between adjacent snippets, and

then uses them to regularize the model with three regularization terms. The experimental results validate that C^3 BN is applicable to various WS-TAL methods with video-level supervision and point-level supervision.

References

- [Belkin *et al.*, 2006] Mikhail Belkin, Partha Niyogi, and Vikas Sindhwani. Manifold regularization: A geometric framework for learning from labeled and unlabeled examples. *Journal of machine learning research*, 2006.
- [Berthelot *et al.*, 2019] David Berthelot, Nicholas Carlini, Ian J. Goodfellow, Nicolas Papernot, Avital Oliver, and Colin Raffel. Mixmatch: A holistic approach to semi-supervised learning. In *NIPS*, 2019.
- [Caba Heilbron *et al.*, 2015] Fabian Caba Heilbron, Victor Escorcia, Bernard Ghanem, and Juan Carlos Niebles. Activitynet: A large-scale video benchmark for human activity understanding. In *CVPR*, 2015.
- [Calway *et al.*, 2015] A Calway, W Mayol-Cuevas, D Damen, O Haines, and T Leelasawassuk. Discovering task relevant objects and their modes of interaction from multi-user egocentric video. In *BMVC*, 2015.
- [Chen *et al.*, 2020] Ting Chen, Simon Kornblith, Mohammad Norouzi, and Geoffrey Hinton. A simple framework for contrastive learning of visual representations. In *ICML*, 2020.
- [Do *et al.*, 2021] Kien Do, Truyen Tran, and Svetha Venkatesh. Clustering by maximizing mutual information across views. In *ICCV*, 2021.
- [He *et al.*, 2020] Kaiming He, Haoqi Fan, Yuxin Wu, Saining Xie, and Ross Girshick. Momentum contrast for unsupervised visual representation learning. In *CVPR*, 2020.
- [Huang *et al.*, 2021] Linjiang Huang, Liang Wang, and Hongsheng Li. Foreground-action consistency network for weakly supervised temporal action localization. In *ICCV*, 2021.
- [Ji *et al.*, 2021] Yuan Ji, Xu Jia, Huchuan Lu, and Xiang Ruan. Weakly-supervised temporal action localization via cross-stream collaborative learning. In *ACMMM*, 2021.
- [Jiang *et al.*, 2014] Y.-G. Jiang, J. Liu, A. Roshan Zamir, G. Toderici, I. Laptev, M. Shah, and R. Sukthankar. THUMOS challenge: Action recognition with a large number of classes, 2014.
- [Ju *et al.*, 2021] Chen Ju, Peisen Zhao, Siheng Chen, Ya Zhang, Yanfeng Wang, and Qi Tian. Divide and conquer for single-frame temporal action localization. In *ICCV*, 2021.
- [Kim *et al.*, 2020] Sungnyun Kim, Gihun Lee, Sangmin Bae, and Se-Young Yun. Mixco: Mix-up contrastive learning for visual representation. *arXiv preprint arXiv:2010.06300*, 2020.
- [Laine and Aila, 2017] Samuli Laine and Timo Aila. Temporal ensembling for semi-supervised learning. In *ICLR*, 2017.
- [Lee and Byun, 2021] Pilhyeon Lee and Hyeran Byun. Learning action completeness from points for weakly-supervised temporal action localization. In *ICCV*, 2021.
- [Lee *et al.*, 2020] Pilhyeon Lee, Youngjung Uh, and Hyeran Byun. Background suppression network for weakly-supervised temporal action localization. In *AAAI*, 2020.
- [Lei and Todorovic, 2018] Peng Lei and Sinisa Todorovic. Temporal deformable residual networks for action segmentation in videos. In *CVPR*, 2018.
- [Liu *et al.*, 2021] Ziyi Liu, Le Wang, Qilin Zhang, Wei Tang, Junsong Yuan, Nanning Zheng, and Gang Hua. Acenet: Action-context separation network for weakly supervised temporal action localization. In *AAAI*, 2021.
- [Luo *et al.*, 2021] Wang Luo, Tianzhu Zhang, Wenfei Yang, Jingen Liu, Tao Mei, Feng Wu, and Yongdong Zhang. Action unit memory network for weakly supervised temporal action localization. In *CVPR*, 2021.
- [Ma *et al.*, 2020] Fan Ma, Linchao Zhu, Yi Yang, Shengxin Zha, Gourab Kundu, Matt Feiszli, and Zheng Shou. Sf-net: Single-frame supervision for temporal action localization. In *ECCV*, 2020.
- [Min and Corso, 2020] Kyle Min and Jason J Corso. Adversarial background-aware loss for weakly-supervised temporal activity localization. In *ECCV*, 2020.
- [Narayan *et al.*, 2021] Sanath Narayan, Hisham Cholakkal, Munawar Hayat, Fahad Shahbaz Khan, Ming-Hsuan Yang, and Ling Shao. D2-net: Weakly-supervised action localization via discriminative embeddings and denoised activations. In *ICCV*, 2021.
- [Robinson *et al.*, 2020] Joshua David Robinson, Ching-Yao Chuang, Suvrit Sra, and Stefanie Jegelka. Contrastive learning with hard negative samples. In *ICLR*, 2020.
- [Sohn *et al.*, 2020] Kihyuk Sohn, David Berthelot, Chun-Liang Li, Zizhao Zhang, Nicholas Carlini, Ekin D Cubuk, Alex Kurakin, Han Zhang, and Colin Raffel. Fixmatch: Simplifying semi-supervised learning with consistency and confidence. In *NIPS*, 2020.
- [Verma *et al.*, 2019] Vikas Verma, Alex Lamb, Christopher Beckham, Amir Najafi, Ioannis Mitliagkas, David Lopez-Paz, and Yoshua Bengio. Manifold mixup: Better representations by interpolating hidden states. In *ICML*, 2019.
- [Yang *et al.*, 2021] Wenfei Yang, Tianzhu Zhang, Xiaoyuan Yu, Tian Qi, Yongdong Zhang, and Feng Wu. Uncertainty guided collaborative training for weakly supervised temporal action detection. In *CVPR*, 2021.
- [Zhang *et al.*, 2018] Hongyi Zhang, Moustapha Cisse, Yann N Dauphin, and David Lopez-Paz. mixup: Beyond empirical risk minimization. In *ICLR*, 2018.
- [Zhang *et al.*, 2021] Can Zhang, Meng Cao, Dongming Yang, Jie Chen, and Yuexian Zou. Cola: Weakly-supervised temporal action localization with snippet contrastive learning. In *CVPR*, 2021.
- [Zhou *et al.*, 2019] Xingyi Zhou, Dequan Wang, and Philipp Krähenbühl. Objects as points. *arXiv preprint arXiv:1904.07850*, 2019.